Recent Advances in Carbon Nanotube-Modified Polylactide

Tao Qiang* and Shibo Jia

School of Materials Science and Chemical Engineering, Xi'an Technological University, Xi'an 710021, China

Abstract: Polylactide (PLA) has been regarded as one of the most promising bio-based, environmentally-friendly polymers. The products derived from PLA will degrade into CO_2 and H_2O ultimately after being wastes. To this extent, PLA is the really sustainable synthetic polymers, due to its nature-to-nature loop within life cycle. However, inherent brittleness, poor heat resistance, slow crystallization rate and high cost, have limited pure PLA and its composites' potential applications. Carbon nanotubes (CNT) is one kinds of one-dimensional nano-materials with hollow structures composed of only hybrid sp^2 C-C bonds. CNT is identified as the most preferred candidate for space elevators, due to its excellent mechanical properties and electrical conductivity. CNT/PLA blends will exert synergistic effects of their individual component, bring breakthroughs in their structures and various properties, and open up potential application scenarios for the resultant composite materials. In this review, recent advances on fabrication methods, structure manipulation, property optimization and application scenarios of CNT/PLA composites were summarized. Especially, the effects of CNT content and pretreatment methods on the microstructures and properties of the resultant PLA composites were focused on in this review. Also, future prospective of CNT/PLA composite materials were addressed.

Graphical Abstract

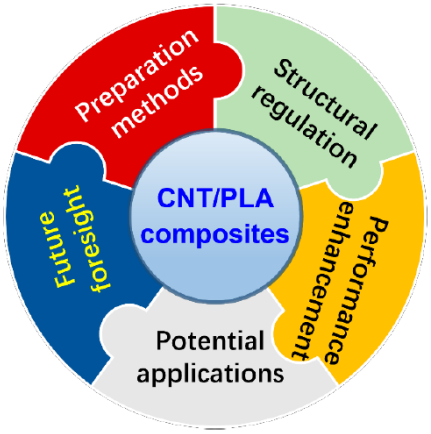

Keywords: Polylactide, Carbon nanotubes, Structure manipulation, Property optimization, Synergistic effects.

INTRODUCTION

In the past decades, global citizen has paid more and more attention to ecological environment, biodiversity and sustainable development, due to the overproduction and overconsumption of petroleum-derived polymers [1]. In this context, various bio-based, degradable, eco-friendly polymers have been developed to replace the traditional petroleum-based polymers in both academia and industry [2, 3].

Among all the biopolymers, polylactide (PLA), the so-called 'corn plastic', was regarded as the most promising eco-friendly biodegradable polyester that derived from renewable resources such as corn, sugar beet and cassava. Thus, the products made of PLA will completely degrade into CO_2 and H_2O under both *in vivo* and composting conditions after being waste. PLA has excellent physical properties, such as outstanding biocompatibility, excellent transparency, high strength and modulus. So, in recent years PLA has been used in various fields, such as tissue engineering, 3D printing and biomedicine. However, PLA is a kind of hard and brittle polyester at ambient temperature. The inherent brittleness, poor heat resistance, slow crystallization rate and high cost, have limited the potential applications of pure PLA and its composites in some emerging fields, such as wearable electronic devices, supercapacitors, and friction nanogenerators [4-7]. In this case, toughening modification, heat resistance improvement and crystallization rate

*Address correspondence to this author at the No. 2, Middle Xuefu Road, Weiyang College Park, Xi'an, 710021, China; Tel: +86-29-8617-3324; Fax: +86-29-8617-3324;
E-mail: qiangtao2005@163.com or qiangtao@xatu.edu.cn

E-ISSN: 2311-8717/24

enhancement are very essential for PLA to widen its application scenarios, beyond some basic research to pristine PLA [8]. Also, PLA has stereoisomers, including poly(L-lactide) (PLLA), poly(D-lactide) (PDLA), and poly(D, L-lactide) (PDLLA) [9].

Carbon nanotubes (CNT) discovered in 1991, has been recognized as the most magical one-dimensional nano-materials in the past decades, due to its low density, high aspect ratio, hollow structure, excellent mechanical and electrical performance [10]. CNT is classified into single-walled carbon nanotubes (SWCNT) and multi -walled carbon nanotubes (MWCNT), according to its different layer number. Up to now, CNT has been confirmed by innumerable scientific reports to improve the components, physical and chemical properties for various polymers to produce versatile advanced composite materials [11, 12].

In recent years, meaningful attempts and important progress have been made to modify PLA with CNT and further explore the potential applications of the resultant CNT/PLA blends or composites in biomedicine, thermal management, conductive materials and e-skins [13-15]. In this review, recent advances of CNT/PLA composite materials are reviewed, with a focus on the preparation, microstructure, property regulation and application in the past five years are reviewed, and their future development prospects are also prospected.

1. PREPARATION METHODS

PLA composites with different types of fillers, various microscopic structures and versatile functions and properties can be made by melt blending, solution blending, and in situ polymerization [13]. A suitable method is very important to prepare the CNT/PLA composites with controllable structures and desired properties. So, the effects of preparation methods on the microstructure control and property enhancement of the resultant CNT/PLA composites are summarized and evaluated at first.

1.1. Melt Blending

Melt blending is a conventional process to prepare polymer blends or composites after different components were heated to the viscous flow temperature of polymeric matrix under shear force [5, 6]. However, sometimes fillers or modification agents can't be uniformly dispersed within the matrix, especially when the filler size is micro - or nano-scale.

The tensile strength and elongation at break of the PLA/MWCNT composites with 1.0 wt% of MWCNT prepared by melt blending method were increased by 18.4% and 12.6%, respectively, compared with that of pure PLA [16]. Zhou *et al* [17] reported that the tensile strength, elongation at break, and impact strength of the CNT-COOH/PLA composite with 0.5 wt% of CNT-COOH were increased by 8.3%, 49.3% and 78.7%, respectively. In addition, its glass transition temperature increases from 82.2 °C (*i.e.*, pure PLA) to 85.3 °C, as shown in Figure **1**.

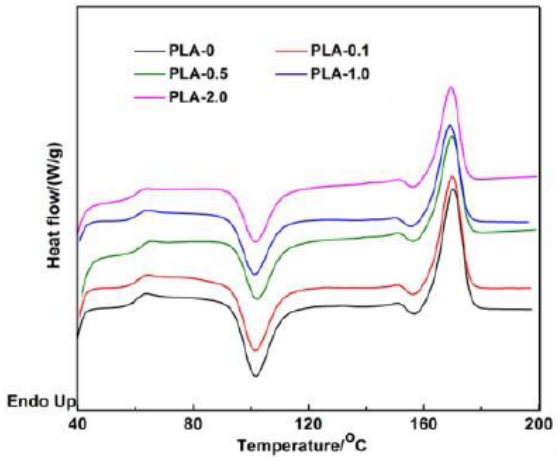

Figure 1: DSC curve of CNT-COOH /PLA composites [17].

1.2. Solution Blending

Solution blending is another common preparation method used to prepare polymer composites. This method has simple process, easy to operate and adjust parameters. So, it is widely used to prepare new polymer composites with expected structures and properties [18].

1.2.1. Solution Casting

Nayara *et al* [19] prepared a PLA/BG/MWCNT film by solution casting. PLA was added to the biofilm (BG) solution and stirred for 60 min after BG was stirred and ultrasound for 15 min at 40 °C. Then, the solution was cast in a mold with the diameter of 9 mm to obtain composite film after drying. The porous PLA/BG/MWCNT membrane with 1.5 wt% of CNT could inhibit the growth for all the types of microorganisms. Yang *et al* [20] prepared the PLLA/PDLA blends (LD) and MWCNT/PLLA/PDLA nanocomposites by solution casting and found DMF is easier to form steric crystals, as shown in Figure **2**.

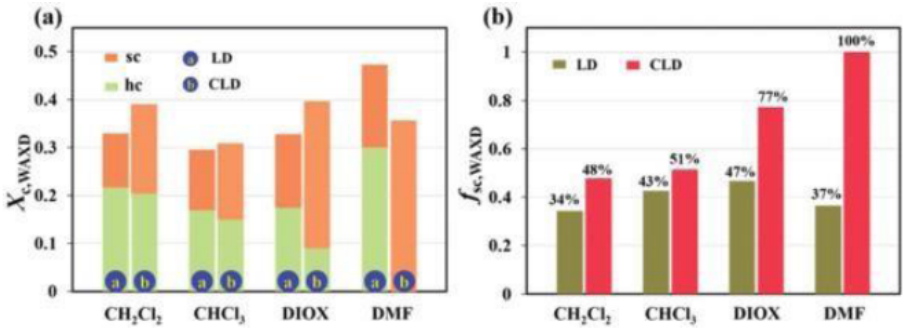

Figure 2: Crystallinity (**a**) and relative content of SC crystals (**b**) in LD and CLD samples cast with different solvents [20].

1.2.2. Solvent Evaporation

The PLA/poly(ε-caprolactone) (PCL) solution and MWCNT/cinnamaldehyde (CIN) ultrasonic dispersion s with dichloromethane (DCM) as solvent were prepared. Then, the solution was mixed, poured into a mold and evaporated to form the PLA/MWCNT/CIN composite film. The results showed that addition of CNT and CIN improved the UV resistance of the resultant composite film: the transmittance decreased by 100% within the wavelength range of 100 -320 nm [21]. Yu *et al* [22] prepared the PLA composites modified with both CNT and cellulose nanocrystal (CNC) by combining Pickering emulsion with solvent evaporation. Its electromagnetic shielding efficiency reaches up to 41.8 dB for the ternary PLA composite with 4.3 wt % of CNT. As shown in Figure **3**, its electrical conductivity reaches up to 59 s/m at this CNT concentration.

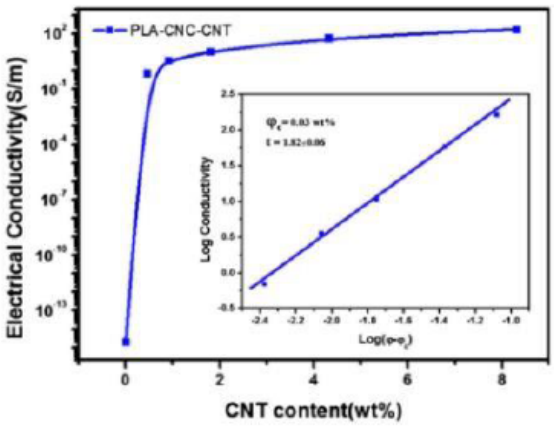

Figure 3: Electrical conductivity of PLA/CNC/CNT composites [22].

1.3. In-Situ Polymerization

During an in-situ polymerization, reactive monomer (or its soluble prepolymer) is added to the dispersed or continuous phase with catalyst. The monomer pre-polymerizes at first after the reaction begins. Then, the pre-polymers begin to polymerize. The final polymer will deposit on the surface of core material with the increasing size.

Li *et al* [23] prepared the PLA composites modified with carboxyl-functionalized COOH-MWCNTs was prepared via in-situ polymerization. The results showed that, glass transition temperature (Tg) of the resultant PLA composite teaches up to 74 °C with 0.5 wt% of COOH-MWCNTs, which is 48 % higher than that of pure PLA (50 °C). Wang *et al* [24] prepared porous PLA/CNT/PANI (polyaniline) (P-PCP) unsupported flexible films by combining in-situ chemical oxidation polymerization of aniline with rapid-mixing chemical oxidation polymerization technique. When aniline concentration is 0.1 mol/L, tensile strength of the ternary PLA composite film reached up to 18 MPa after heat treatment at 60 °C for 60 min (P-PCP-H-1, see Figure **4** (**a**)). What's more, its capacitance retention is kept as high as 93.4% after been 180° bended for 700 times, as shown in Figure **4** (**b**).

1.4. Mechanochemical Method

Mechanochemistry is an emerging s technique to investigate physical, chemical, biochemical or physicochemical changes of substances, which will exert strong 3D shear forces to realize the solid phase synthesis of matter [25]. Now, it has been widely used to modify solid materials, synthesize functional polymers and develop various composite materials [26, 27]. The CNT/PLA composite materials were prepared via mechanochemical method. The crystallinity of the resultant CNT/PLA composites reaches up to 33.28 % (*i.e.*, 3.06 times that of the un-treated counterparts, 10.87%) when the CNT content is 1.0 wt% [28].

1.5. 3D Printing

3D printing is an additive manufacturing technique for rapid prototyping, which has been used to

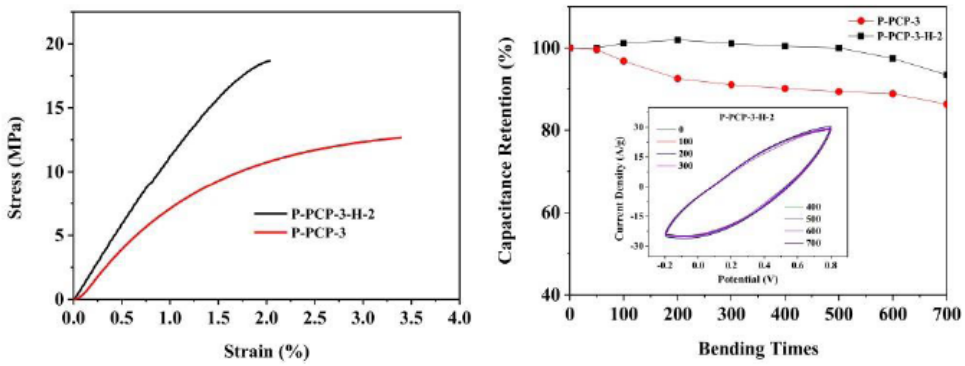

Figure 4: Stress-strain curves (**a**) and flexible stability of the composite film electrodes (**b**) of P-PCP-3 and P-PCP-3-H-2 composite films [24].

prototype various mechanical parts and composite materials [29-31].

The MWCNT/PLA composites were successfully manufactured via an electric- field-driven (EFD) fusion jetting 3D printing method [32]. Its conductivity of the resultant composites is 10^{-8} and 10^{-6} S/cm, respectively, when 2.0 and 5.0 wt% of MWCNT were added in PLA under the frequency of 10^{6} Hz. As the preparation process shown in Figure **5**, PLA particles were mixed with hybrid graphene nanosheets (GNPs) and CNT to produce the PLA/GNPs/CNTs printing parts via 3D printing technique [33]. The tensile strength and Young's modulus are 16.2 % and 25.5 % higher than that of pure PLA, respectively.

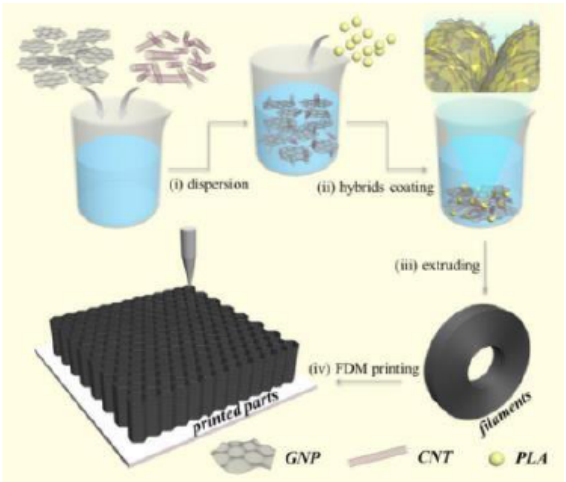

Figure 5: Schematic diagram of 3D printing of PLA/GNPs/CNTs nanocomposites [33].

1.6. Physical Foaming

The chain-extended PLA was prepared by grafting octa(epoxycyclohexyl) polyhedral oligomeric silsesquioxanes (POSS) on CNT for first step [34]. Then, the CNT-POSS/PLA foam was obtained by continuous solid-state foaming at 140 °C and 16 MPa for 5 hours with CO_2 as foaming agent. Its expansion rate is 13 times higher than that of unmodified PLA foam. The CNT/PLA nanocomposite foam with ultra-low density was successfully prepared through straightforward, efficient and green CO_2- based foaming methodology, as the porous morphology shown in Figure **6** [35]. Especially, its volume expansion ratio reached up to 49.6 when 2.0 wt% of CNT was added at 121 °C.

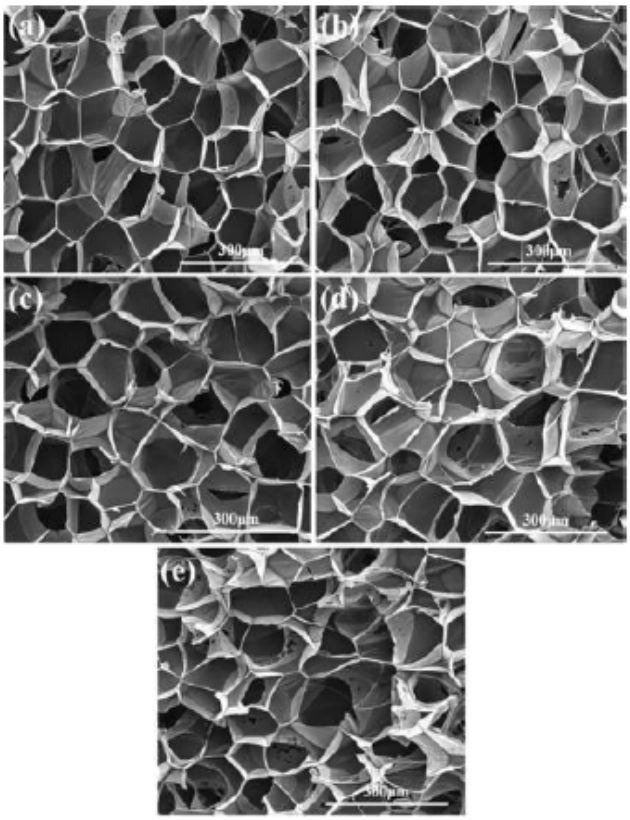

Figure 6: Porous morphology of the PLA/CNTs foams under different foaming temperature: (**a**) 115 °C, (**b**) 118 °C, (**c**) 121 °C, (**d**) 124 °C, and (**e**) 127 °C [35].

2. STRUCTURAL REGULATION

2.1. Chemical Structures

Hydrogen bonds exist within the PLA composites modified with nitrogen-doped carbon nanotubes (N-CNT), due to nitrogen-hydrogen interactions [36]. Moderate and weak hydrogen bonds are dominant at low temperature (-73 °C to -23 °C), while strong hydrogen bond appears at temperature above zero (0 to 50 °C). Also, reduction- graphene oxide/PLA/CNT (RGO/CNT/PLA) nanocomposites show hydrogen bonds formed between the RGO or CNT groups and the C=O groups of PLA chains [37], as shown in Figure **7**.

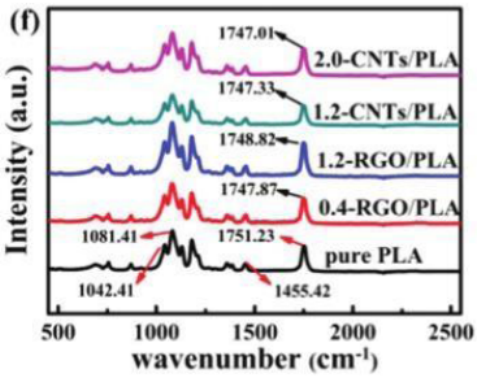

Figure 7: FTIR spectra of PLA nanocomposites with different RGO or CNT concentrations [37].

2.2. Dispersibility of CNT in PLA

Interfacial adhesion between CNT and matrix can be improved by CNT's chemical or physical modification. What's more, it is beneficial to the uniform dispersion of CNT in polymer matrix. Sodium dodecyl benzene sulfonate (SDBS) was used to non- covalently modify MWCNTs in order to prepare SWCNTs/PLLA composites. The result shows that there has no agglomeration of MWCNT occurred in PLLA matrix until its filling content increased to 3.0 wt% [38].

In addition, 3D printing process helps to evenly disperse nano-filler in polymer matrix. As shown in Figure **8**, MWCNT can evenly distribute in PLA matrix, when its content increased up to 5 wt% [32].

2.3. Micro-Scale Structures

Usually, some changes on macromolecular chains, chain segments, configurations and conformations will occur when two different polymers are mixed into together. Their intrinsic properties and interactions between different components will have some effects on the appearance, structures and properties of the resultant mixture or blends.

MWCNT can be uniformly dispersed in PLA matrix subjected to 3D printing composites [39]. The fine structure of CNT can be observed when its content is 1.5

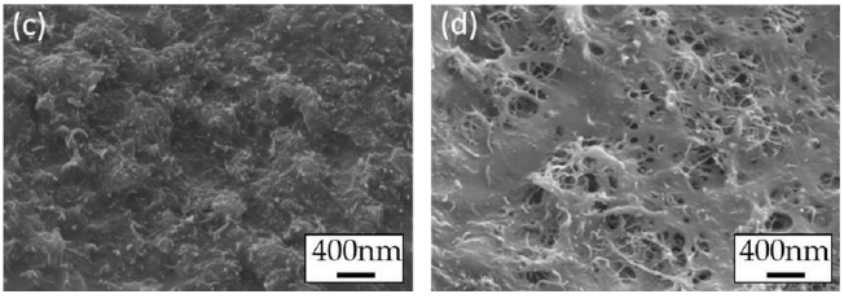

Figure 8: SEM photos of PLA composites with 2.0 (**a**) and 5.0 (**b**) wt% of MWCNT [32].

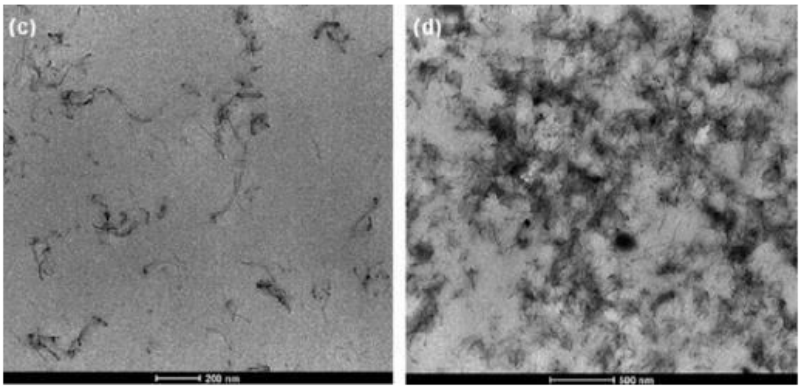

Figure 9: TEM photos of the PLA composites with different MWCNT: (**c**) 1.5 wt% and (**d**) 9 wt% [39].

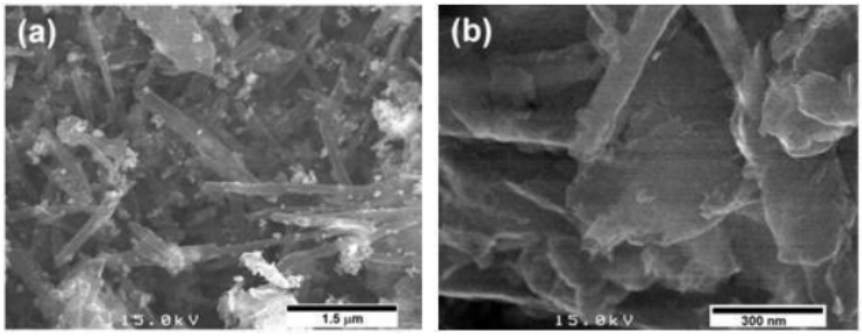

Figure 10: SEM photos of CNT/PLA (**a**) and CNT/PLA/Pd (**b**) composites [40].

wt% under transmission electron microscope (TEM). More interesting, MWCNT begins to partly agglomerate when its content reached up to 9 wt%, as shown in Figure **9**.

By grafting PLA to CNT and fixing palladium (Pd) nanoparticles, the CNT/PLA and CNT/PLA/Pd composites show a layered structure with Pd nanoparticles distributed on CNTs/PLA surface [40], as shown in Figure **10**.

2.4. Crystalline Structures

Cylindrical fibers and spherulites can be observed in pure PLA and CNT/PLA nanocomposites prepared by solvent evaporation method under atomic force microscope (AFM) [36]. The average diameter of fiber and spherulite is 17.2 and 32 nm, respectively. There are larger spherulites with a diameter of 124 nm in the composite, though its spherulite number is less than that of pure PLA, as shown in Figure **11**. The PLA/CNT@LDH (layered double hydroxides) membranes was prepared by electrospinning technology. The average size of PLA spherulites slightly decreases with the increase of CNT@LDH content, while the number of spherulites increases [41].

3. PERFORMANCE OPTIMIZATION

3.1. Thermal Properties

3.1.1. Heat Deflection Temperature

Low heat deflection temperature (HDT) is one of the intrinsic limitations that limits the potential application scenarios for PLA. At the same time, it has been one of the hottest topics for PLA modification. The CNT/PLA composite was prepared by aqueous cross-linking reaction, with CNT content of 1.0 part per hundreds of resins (phr). After cross-linking in aqueous phase for 7 hours, HDT of the resultant MWCNT/PLLA increased to 106 °C, which is 70.9% higher than that of non-cross- linked PLLA (62 °C) [42]. Vapor-grown carbon

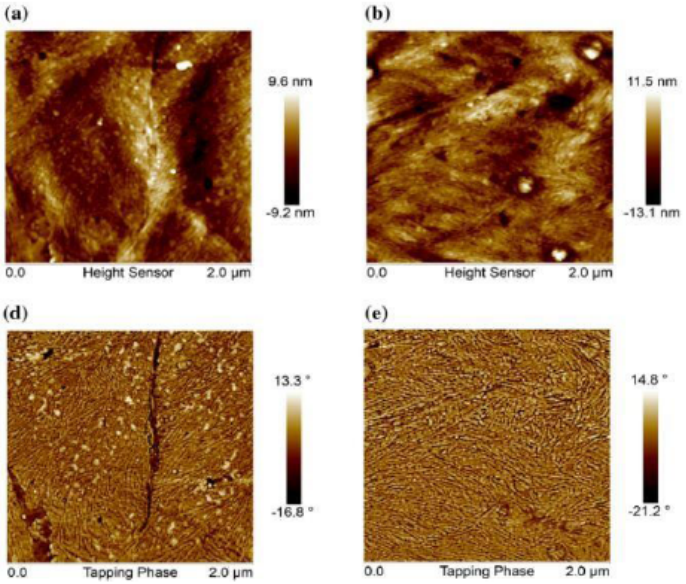

Figure 11: AFM photographs of pure PLA and PLA/CNT composites [36].

nanofiber (VGCF) was functionalized for the first step. Then, PLA was grafted on the surface of VGCF in order to prepare PLA-g-VGCF/PLA nanocomposites by melting composite method. The results showed that, with 10wt% of PLA-VGCF, the HDT of PLA-g-VGCF/PLA composite is as high as 139 ℃, much higher than that of pristine VGCF/PLA [43], as shown in Figure **12**.

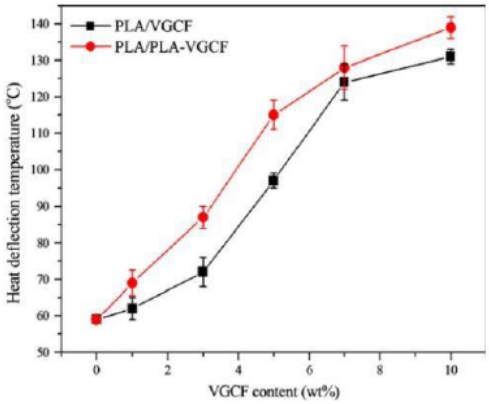

Figure 12 Relationship between HDT and VGCF content for its PLA nanocomposites [22].

3.1.2. Glass Transition Temperature

Glass transition temperature (Tg) of the CNT/PLA composite fiber prepared by electrospinning process increased to 63 °C, when 0.5 wt% of CNT was added [44]. Vu [45] Ternary PLA/CNT composites modified with dispersed orange 3 (DO3) was prepared by a two-step method: solution mixing combined with compression molding. As the DSC curves shown in Figure **13**, Tg of the PLA/CNT/DO3 composite is 52.3 °C when 0.05 wt% of CNT was added, 1.8 °C higher than that of CNT/PLA composite (50.5 °C). When the CNT content increased to 0.1 wt%, Tg of the CNT/PLA and PLA/CNT/DO3 composites were enhanced to about 54 °C.

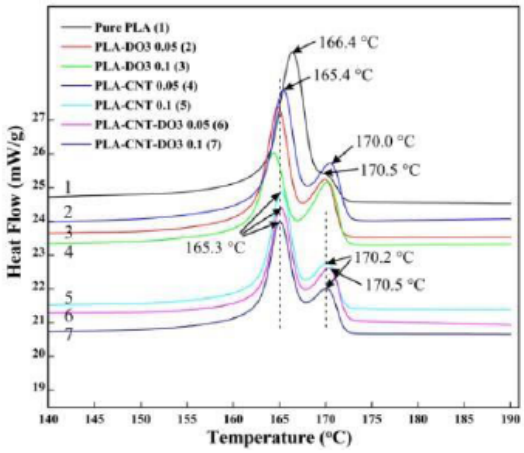

Figure 13: DSC curves of pure PLA and PLA nanocomposites [45].

3.1.3. Melting Behavior

PLA nonwovens coated with MWCNT were prepared by electrostatic spinning show melt temperature of 147-148 °C and enthalpies of melting of 21-24 J/g [46]. CNT- POSS will change PLA's crystalline structure and increase its melting temperature. As the DSC curves shown in Figure **14**, melting temperature of the CNT-POSS/PLA foam reached to 157 °C by adding 1.0 phr of CNT-POSS, which is 3.2% higher than that of pure PLA (152 °C) [34].

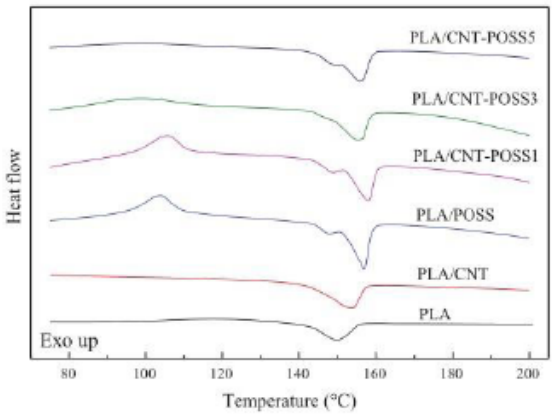

Figure 14: DSC curve of PLA foam [34].

3.1.4. Crystallization

Slow crystallization rate is another intrinsic limitation that greatly limits many potential applications of PLA, such as flexible electronics and smart wearables. Therefore, accelerating the crystallization rate of PLA is another research hotspot at both domestic and international level in recent years. Adding nucleating agent has been regarded as one of the most important strategies to increase polymer's crystallization rate. MWCNTs incorporation le ads to an enhanced crystallization for PLA. The crystallinity of PLA increases to 12.5 % with 10 wt% of MWCNT, demonstrating a 54.3% increase over the crystallinity of 1.0 wt% MWCNT composites (8.1%) [47].

Also, CNT was modified with hydroxy-ended hyperbranched polyester (HBP- H_2O_2) to prepare CNTs-H_2O_2/PLLA composite sheets [48]. The results showed that the CNT/PLA composite has the narrowest crystallization peak, followed by the CNTs-H2O2 crystallization peak and PLLA is the widest, as shown in Figure **15**.

3.1.5. Thermal Stability

The temperature at 5% weight loss (T5) of for the CNT/PLA composites prepared by melt blending

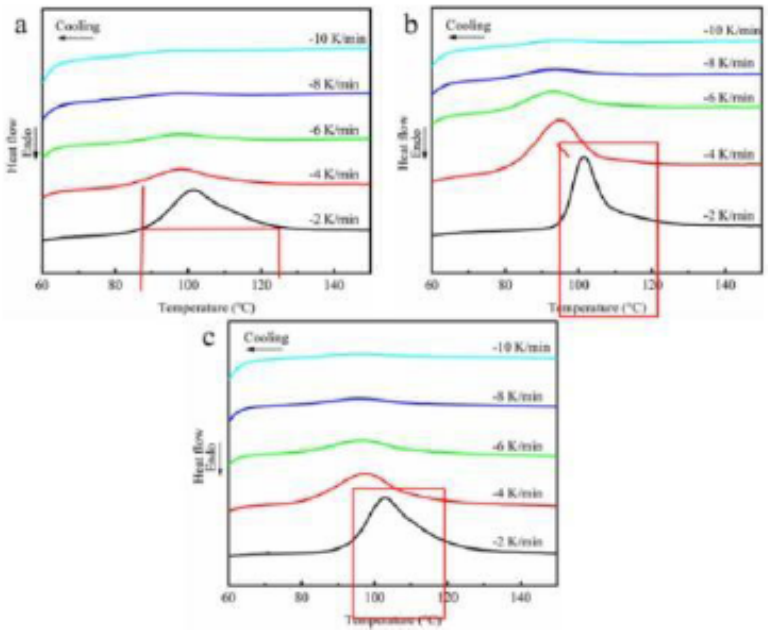

Figure 15: DSC cooling curves of PLLA (**a**), PLLA/CNTs (**b**) and PLLA/CNTs-H2O2 (**c**) at different cooling rates [48].

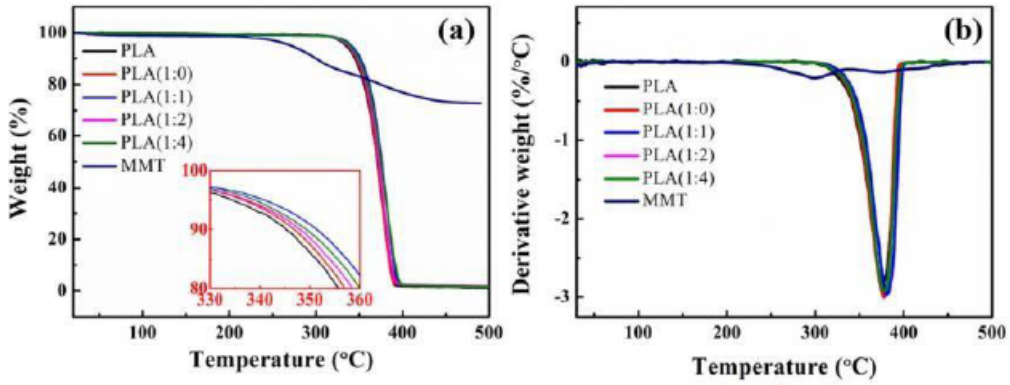

Figure 16: TGA (**a**) and DTG (**b**) curves of MMT, PLA and their nanocomposites [49].

method is 3.0 °C higher than that of pure PLA [49]. The initial decomposition temperature of PLA/polyethylene oxide/CNTs (PLA/PEO/CNTs) nanocomposites increased up to 258 ℃ with 60 wt% of PLA, 40wt % of PEO and 1.0 wt% of CNTs, respectively [50]. It illustrates a 3.2 % of increase, compared with their unmodified counterparts (250 °C). It shows that the addition of CNT can improve the thermal stability of PLA composites.

3.2. Mechanical Properties

3.2.1. Tensile Strength

PLA is a hard-and-brittle aliphatic polyester at ambient temperature. Its intrinsic brittleness restricts PLA's potential applications in many emerging fields.

PLLA/CNT nonwovens were prepared with oligomeric linear ladder poly(silsesquioxane)s (LPSQ) as modification agent by electrospinning technology. Tensile strength of the resultant nonwovens is 2.4 times higher than that of pure PLLA when 10 wt% of LPSQ-COOMe and 0.1 wt% of CNT were added (see Figure **17**). It illustrates CNT has excellent performance when it was used to modify PLA [51]. Compared with that of pure PLA, tensile strength and stiffness of the PLA/graphene nanosheets/CNTs (PLA/GNPs/CNTs) ternary composites increased by 44% and 66%, respectively, when 0.5wt% of CNT and GNPs mixed components was added. The results show that different types of nanofillers can improve the mechanical properties of PLA matrix composites via their synergy effects [52].

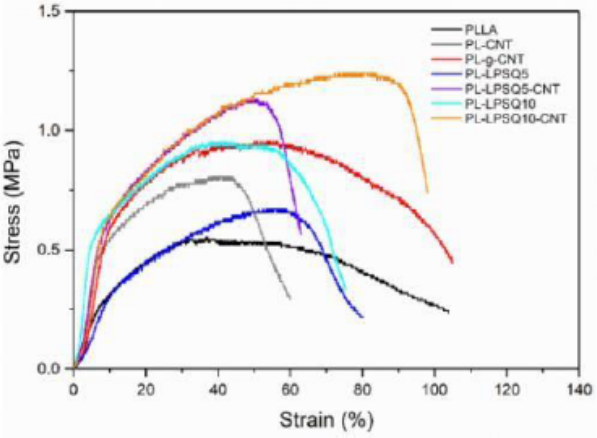

Figure 17: Stress-strain curves of PLA-based nonwovens [51].

3.2.2. Young's Modulus

PLA/ MWCNT/polyethylene glycol (PLA/MWCNT/PEG) composite fibers were prepared by electrostatic spinning process [44]. Young's modulus of the composites reached up to 26.1 MPa with 0.5 wt% of MWCNT and 0.1 wt% of PEG, which is 38.4% higher than that of pure PLA (*i.e.*, 5.39 MPa). Also, PLA/montmorillonite/MWCNT (PLA/MMt/MWCNT) nanocomposites showed multiple enhancement in mechanical properties. With 1.0 phr of MMt/MWCNT, Young's modulus and elastic modulus of the resultant composites increase to 19 GPa and 2.0 GPa [53], as shown in Figure **18**.

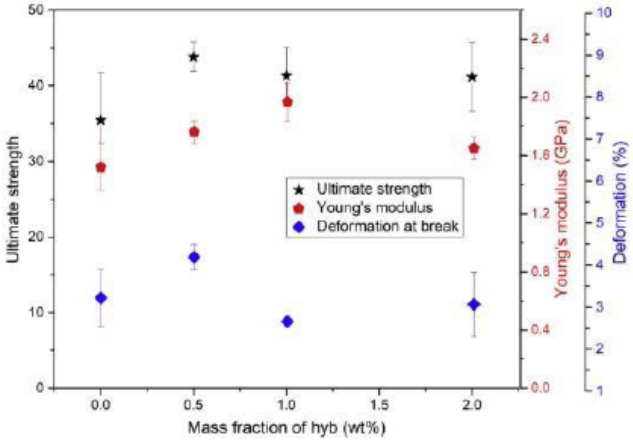

Figure 18: Mechanical properties of PLA and PLA hybrid nanocomposites [53].

3.2.3. Impact STRENGTH

Introducing various elastomers into brittle resins is one of the effective methods to improve its impact strength. Impact strength of the PLA composites was enhanced to 386.36 J/m^2 with 0.5 wt% of CNT via solvent evaporation method, which is 14.5% higher than that of pure PLA [54]. Also, the PLA/polybutylene adipate- terephthalate/CNT (PLA/PBAT/CNT) composites were prepared via melt blending method. The results showed that impact strength of the ternary PLA/PBAT/CNT composites increase by 155% when the PLA/PBAT ratio is 60/40 blending with 3wt % of CNT (Figure **19**) [55].

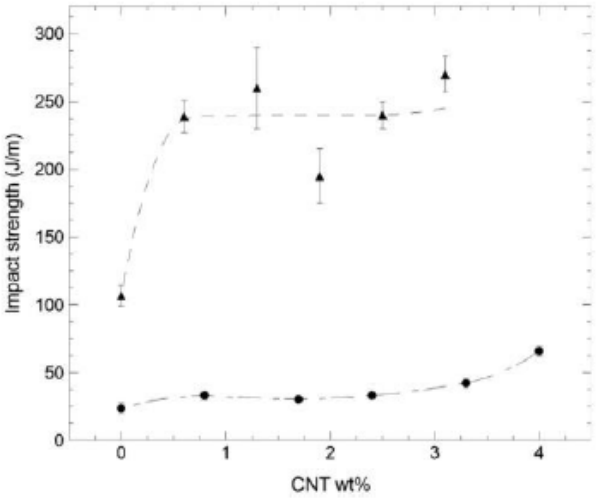

Figure 19: Impact strength of the PLA composites with different CNT content and PLA:PBAT ratios: (●) 80:20, (▲) 60:40 [55].

3.2.4. Elongation at Break

Elongation at break is an important parameter to evaluate materials' toughness. The PCL/PLA composites modified with 0.5 wt% of CNT/MMT increased its elongation at break and tensile strength of the resultant composites by 137.4% and 79.6%, respectively [56]. The 3-aminopropyltriethoxysilane (KH550) was grafted onto worm-like helical carbon nanotubes (HCNT) to prepare HCNT-KH550/PLA composites, which showed a 205% increase in elongation at break compared to pure PLA [57], as shown in Figure **20**.

3.2.5. Brittle-Tough Transition

For PLA, glass transition temperature (Tg) is a key index to illustrate its transition from glassy to highly elastic state, which will directly affect the processing temperature window and properties of the resultant PLA blends or composites.

The propylene/ethylene-propylene-diene/CNT (PP/EPDM/CNT) composites was prepared by melt blending [58]. The results show that the toughening efficiency of CNT is related to the thickness τ of matrix ligament: CNT shows better toughening effect when τ

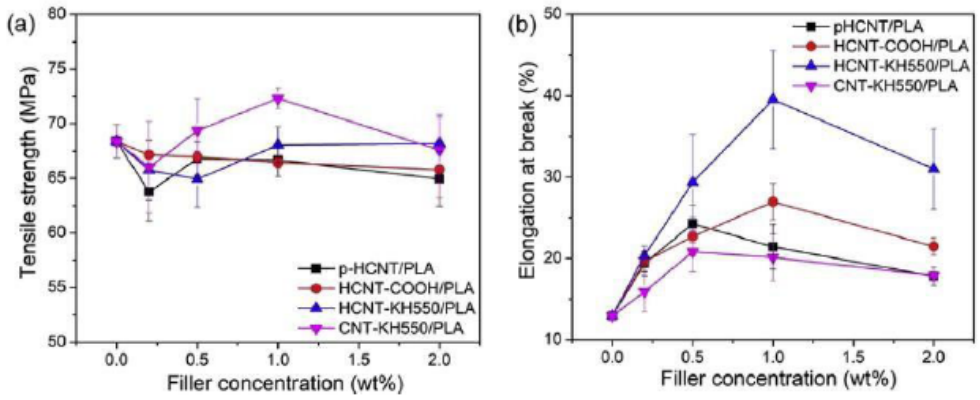

Figure 20: Tensile strength (**a**) and elongation at break (**b**) versus filler amount for untreated, HCNT and CNT treated PLA composites [57].

is in the range of 0.85-1.15 mm. The impact strength of the composites reaches up to 39 kJ/m^2 with 2.0 wt% of CNT. PLLA/polyurethane (PLLA/TPU) blends were modified with CNT to prepare ternary PLLA/TPU/CNTs nanocomposites. With 2.0 wt% of CNT, impact strength of the resultant nanocomposites increase up to 53.7 kJ/m^2 at room temperature, which is 16 times higher than that of pure PLLA and 8 times higher than that of PLLA/TPU blends, respectively [59], as shown in Figure **21**.

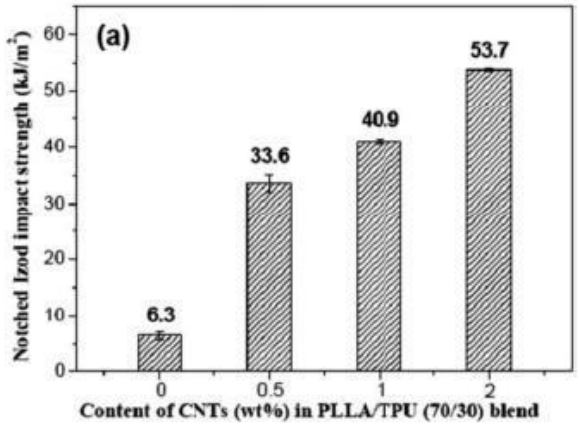

Figure 21: Impact strength of PLLA/TPU blends with different CNT content [59].

3.3. Electrical Conductivity

3.3.1. Conductivity

Carbon nanotubes have excellent electrical conductivity. So, it was used to modify various polymers to prepare conductive polymeric composites [11, 12]. As the SEM picture shown in Figure **22**, MWCNT significantly increased the electrical conductivity of PLA composites with 3.0 wt% of CNT filling: its surface resistivity decreases from 1.95×10^{15} Ω of pure PLA to 2.48×10^6 Ω and volume resistivity decreases from 5.20×10^{15} Ω·cm of pure PLA to 9.98×10^6 Ω·cm, respectively [16].

Also, the electrical conductivity of poly(3-hydroxybutyrate)-3-hydroxyvalerate/CNT/PLA (PHBV/CNT/PLA) composites increased up to 2.79×10^{-2} S/m with only 1.0 wt% of CNT. It means that 1.0 wt% of CNT increases 12 orders of magnitude, compared with that of PLA/PHBV blend (8.679×10^{-14} S/m). The ternary PHBV/CNT/PLA has transformed to semiconducting materials [60].

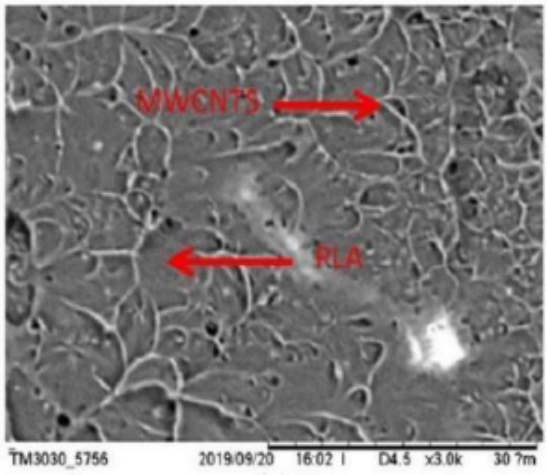

Figure 22: SEM picture of MWCNT/PLA composites [16].

3.3.2. Percolation Transition and Its Mechanism

The PLA/PBAT/MWCNT composites was prepared by premixing MWCNT with PLA and PBAT. Electrical conductivity of the PLA/PBAT/MWCNT composites increased to 1×10^{-1} S·m^{-1} that is 5 magnitudes higher than that of MWCNT/PLA, when the ternary composites were prepared at a 50:50 ratio of PLA to PBAT (Figure **23**) [61]. When the immiscible PLA/poly(ethylene vinyl acetate) (EVA) composites was modified with 1.0 phr

of MWCNTs, its conductivity of the resultant composites increased to 4×10^{-7} S/m [62].

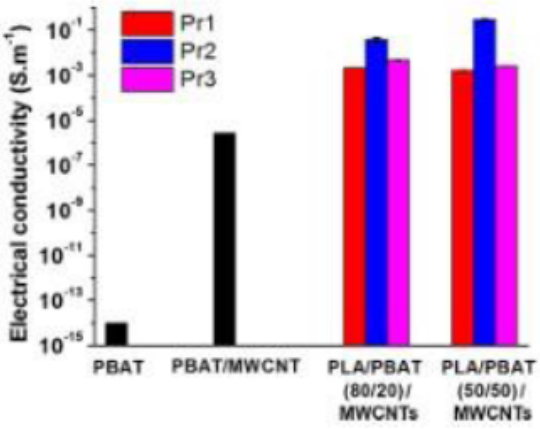

Figure 23: Electrical conductivity of pure PBAT, PBAT/MWCNTs mixture and PLA/PBAT/MWCNTs nanocomposites [61].

3.4. Rheological Properties

The CNTs/PLA nanocomposite foams with ultra-low density was prepared via physical foaming method. The results show that its complex viscosity was enhanced by 2 magnitudes with 2.0 phr of CNT, compared with that of pure PLA, as shown in Figure **24** [35]. Even for the immiscible PLA/EVA composites, its complex viscosity and storage modulus were increased [62].

3.5. Barrier Properties

Conductive polymer composites with low density, excellent conductivity, processability and corrosion resistance, have potentials applications for electromagnetic interference (EMI), due to high shielding effectiveness (SE). The CNT/PLA composites prepared by coating CNT on 3D printed PLA scaffolds showed the interconnected conductive networks after compression. Thus, its EMI SE of the resultant composites increased up to 67 dB with 5.0 wt% of CNT, as shown in Figure **25** [63].

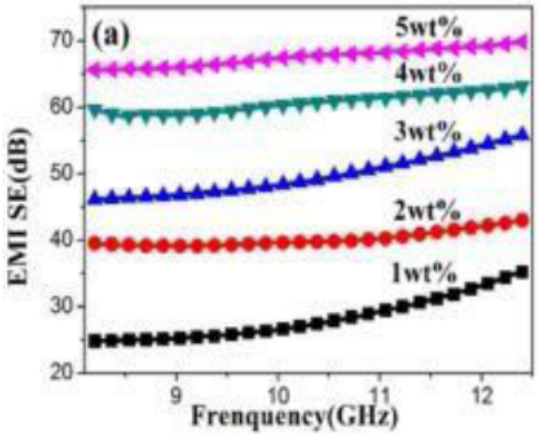

Figure 25: EMI SE of the CNT/PLA composites under different CNT content and frequency [63].

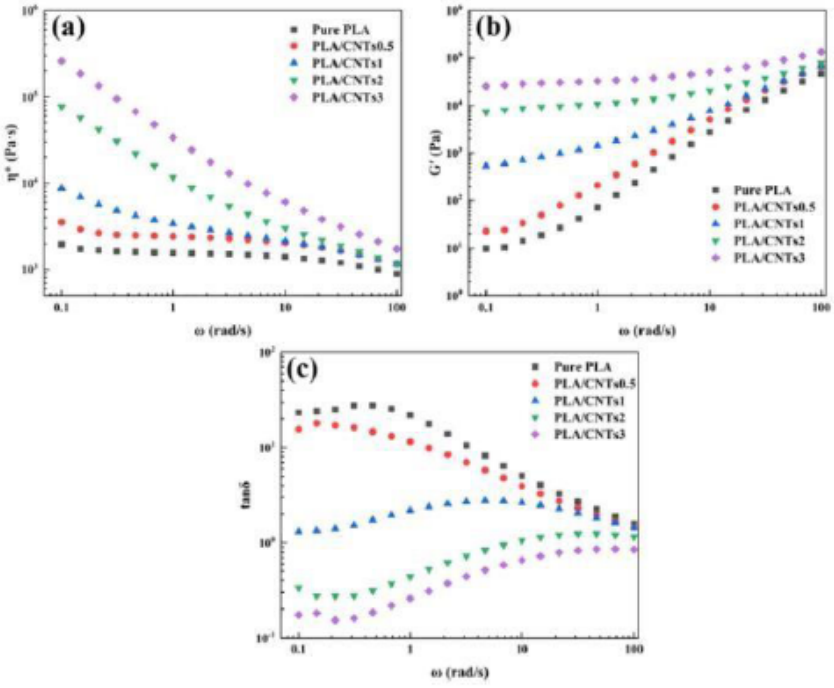

Figure 24: Rheological properties of the CNTs/PLA composites: (**a**) complex viscosity, (**b**) storage modulus and (**c**) dissipation factor (tan δ) [35].

Nitric acid-modified CNTs (N-CNTs)/PLA/PEG composites prepared by melt blending was verified to hinder the loss of volatile degradation products during the thermal decomposition due to nanofiller addition, as the thermal decomposition curves shown in Figure **26**. The initial decomposition temperatures of the CNTs/PLA, PLA/PEG/N-CNTs and PLA/PEG/CNTs composites reached up to 247.3 °C, 267.3 °C, and 285.7 °C, respectively, 1.4%, 9.1% and 16.7% higher than that of pure PLA (244.8 °C) [64].

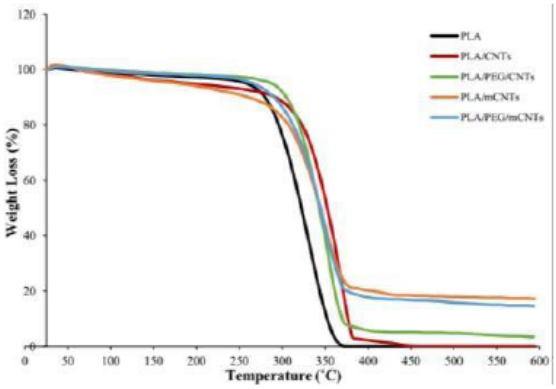

Figure 26: Thermogravimetric curves of pure PLA and its nanocomposites [64].

3.6. Degradation Performance

Mulching film is used to effectively improve crop yields and utilization efficiency of water resource in agricultural fields, beyond maintaining soil moisture, regulating soil temperature and control ling weeds. Nowadays, the mulch used worldwide is mainly made of petroleum-based and non- degradable polyethylene (PE). Waste mulch film caused serious soil pollution and crop yield reduction. In this case, biodegradable mulch (BM) has been paid increasing attention in both academia and industry to solve the plastic pollution from PE mulch film.

The PLA/PBAT films begin to degrade after 60 days and will further degrade into small fragments after 240 days since sowing potatoes [65]. For the CNT/PLA nanocomposite film, CNT will form a zigzag path in the PLA matrix, inhibit water molecules from penetrating into deeper polymer matrix and delay PLA's degradation by hindering mass transfer [66], as shown in Figure **27**. The initial decomposition temperature of pure PLA decreases by 12.2% after degradation treatment for 300 h, while that of the CNT/PLA composites decreases by only 1.0%.

4. APPLICATION SCENARIOS

4.1. Filtering Membranes

The CNT/PLA filtration membrane prepared by electrospinning technology has uniform thickness and smooth surface. Its fiber diameter increases gradually with the increasing CNT content. The CNT/PLA filtration membrane showed excellent hydrophobicity when the mass fraction of CNTs in the spinning solution increased from 0.05% to 0.85%. In addition, filtration efficiency of the CNT/PLA filtration membrane for oily media is higher than that for salt media [67], as shown in Figure **28**. It means that this filtration membrane can quickly separate oil from water.

4.2. 3D Printing Filament

The 3D-printed CNT/PLA composites with excellent EMI was prepared via melting deposition

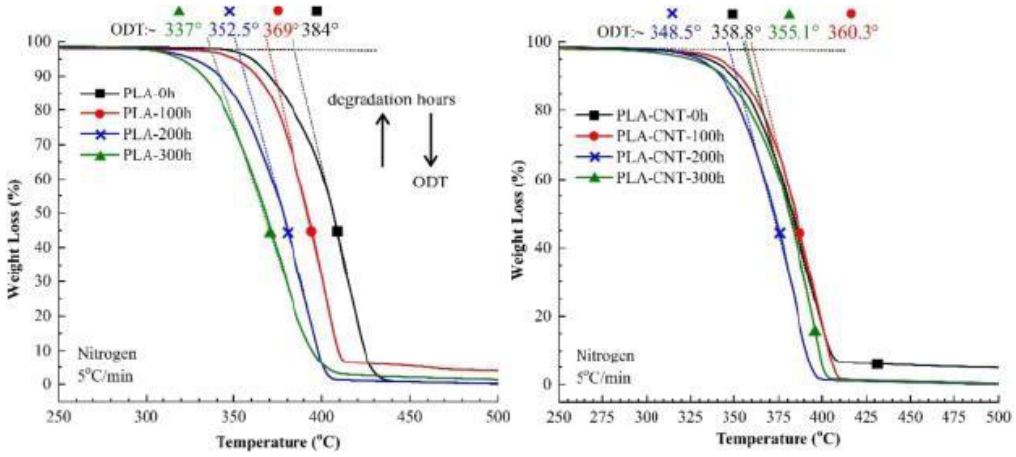

Figure 27: TGA curves of pure PLA (**left**) and PLA nanocomposites with 1.0 wt% of CNT (**right**) after different degradation time [66].

Figure 28: Applications of the PLA/CNTs filtration membrane for oil-water separation: n- hexane/saturated salt water (left) and n-hexane/water (right) [67].

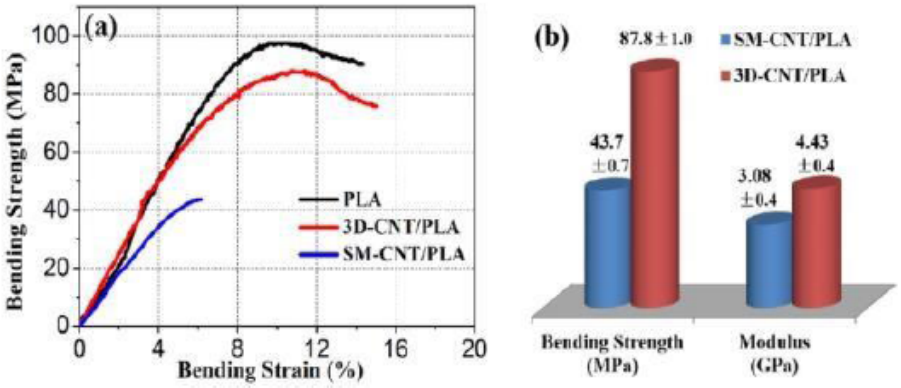

Figure 29: Flexural stress-strain curves (**a**) and bending strength and modulus (**b**) of pure PLA and CNT/PLA composites [63].

[63]. As shown in Figure **29**, its Young's modulus and flexural strength reached up to 4.43 GPa and 87.8 MPa, respectively, 101% and 43% higher than that of their hot-pressed counterparts.

4.3. Biomedical Application

PLA is a bio-based, biodegradable aliphatic polyester. In 1995, PLA was approved by Food and Drug Administration (FDA) to be used as medical surgical sutures, internal fixation materials, tissue repair materials, microcapsules for injection, and controlled-release carriers. Up to now, PLA has been widely used in many biomedical scenarios to replace with non- degradable polymers.

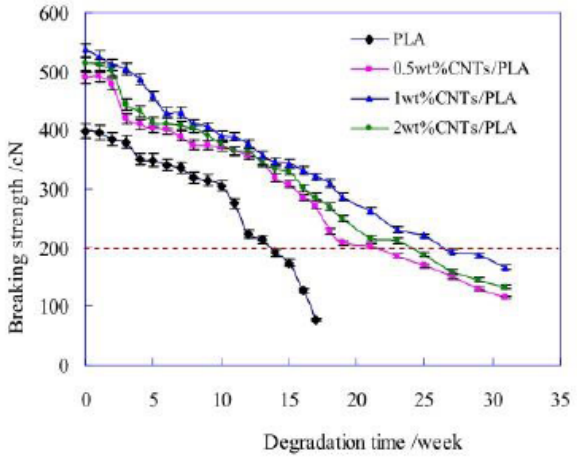

Figure 30: Breaking strength of pure PLA and CNTs/PLA sutures after different degradation time [68].

The medical sutures from CNT/PLA composite filament s were prepared by melt spinning method. Its strength period of the CNT/PLA composite sutures increased to 23.6 weeks, 13.1 weeks higher than that of the unmodified PLA suture. What's more, their breaking strength are superior to that of pure PLA (Figure **30**). It is helpful to enhance the service time of sutures and is advantageous to the healing of wound [68].

4.4. Packing Materials

PLA is bio-based polyester with many merits, such as renewable raw materials and low toxicity. However, its inferior anti-bacterial performance limits PLA's potential applications as packaging materials. CNT and silver nanoparticles (AgNPs) were used to prepare CNTs/AgNPs/PLA nanocomposites by two solvent-assisted methods. The CNTs/AgNPs/PLA composites illustrates higher thermal stability and tensile strength (Figure **31**). Also, the CNTs/AgNPs/PLA nanocomposites show better antibacterial activity to hemolytic staphylococcus, due to the antibacterial properties of AgNPs [69].

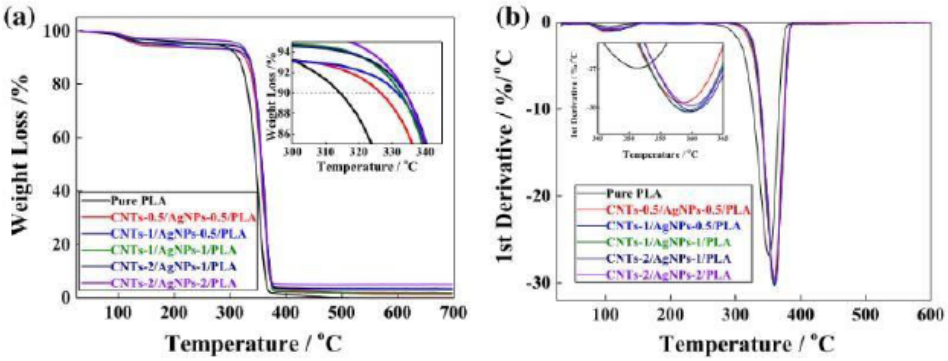

Figure 31: TGA (**a**) and DTG curves (**b**) of pure PLA and CNTs/AgNPs/PLA composites [69].

4.5. Electrode Materials

Nowadays, lithium-ion batteries have been widely used in mobile phones, laptop computers, micro - electromechanical systems and electric vehicles. Honeycomb composite electrode s of PLA/LiFePO4(LFP)/CNT was prepared via combining 3D printing with fuse manufacturing method . The results showed that, the effects of battery thickness on specific capacity can be negated by engineering desired porosity to improve its specific and areal capacity simultaneously (Figure **32**). Specific capacity of the thickest electrode (i.e., 300 µm) increases from 125 m Ahg^{-1} to 151 $mAhg^{-1}$. What's more, there is no loss of areal capacity with the increase of porosity [70].

4.6. Supercapacitors

In recent years, flexible energy storage devices have received more and more attention. Supercapacitors have the advantages of high power of traditional capacitors and high specific energy of batteries. So, supercapacitors mean the most promising candidates for power sources and have promising application prospects for portable electronic devices.

The porous PLA/CNTs nanocomposites was prepared to manufacture degradable flexible and free-standing composite membrane electrodes for supercapacitors by in- situ rapid hybrid chemical oxidative polymerization with aniline. The ternary

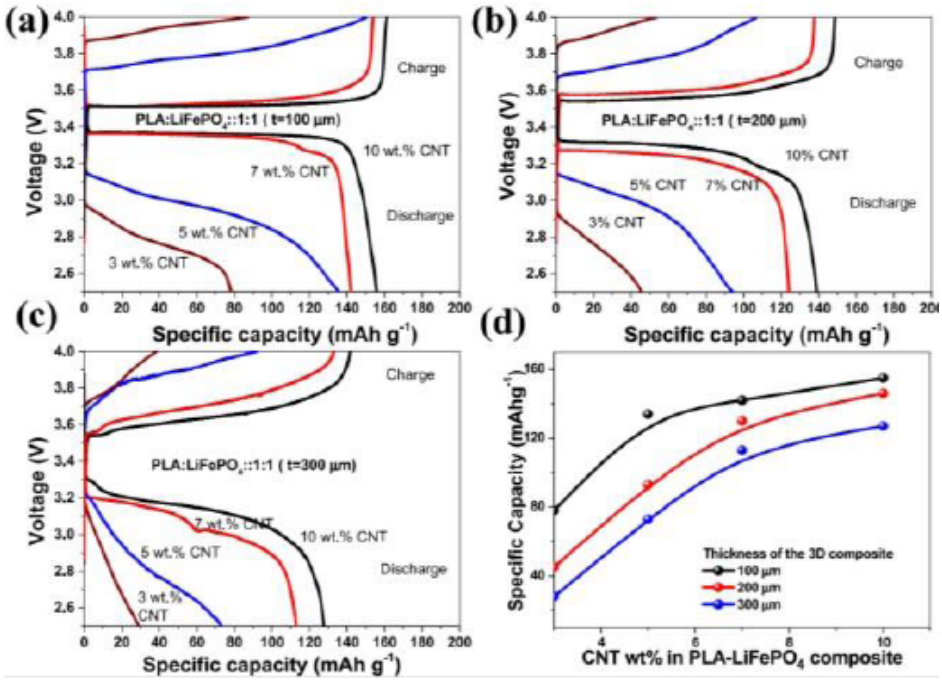

Figure 32: Charge/discharge voltage profiles of the PLA/LFP/CNT electrodes for different thickness: (**a**) 100 µm, (**b**) 200 µm and (**c**) 300 µm, and specific capacities with different CNT content (**d**) [70].

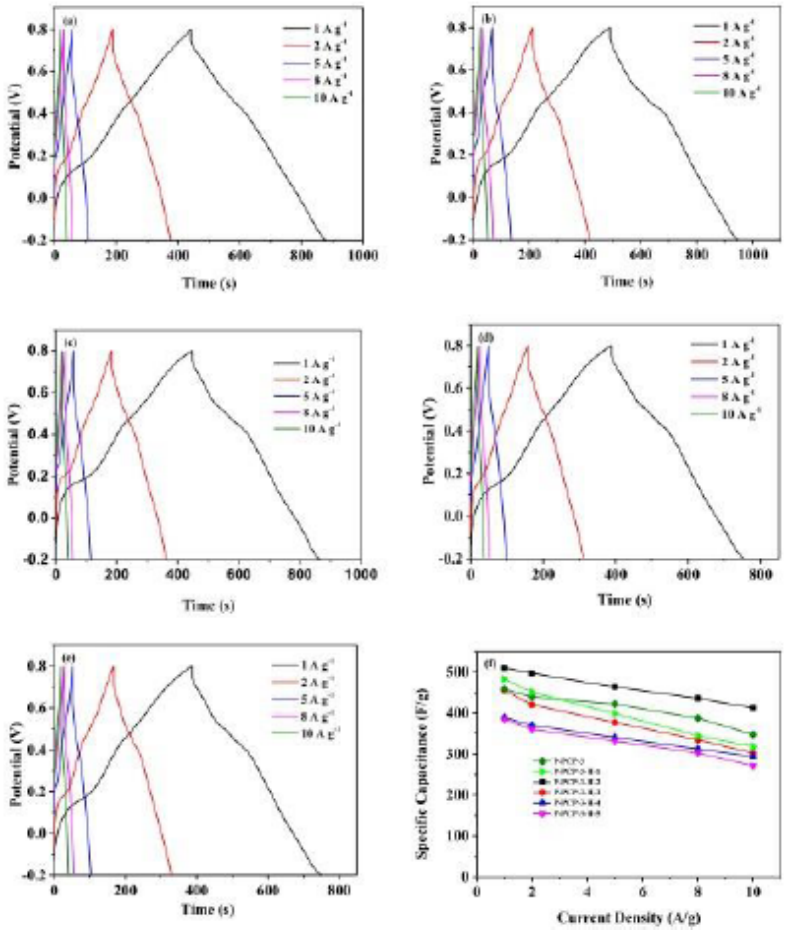

Figure 33: Galvanostatic charge-discharge (GCD) curves of P-PCP-3-H-1 (**a**), P-PCP-3-H-2 (**b**), P- PCP-3-H-3 (**c**), P-PCP-3-H-4 (**d**), and P-PCP-3-H-5 (**e**) and specific capacitance (**f**) at different current density [24].

PLA/CNT/PAN membrane electrode has longer discharge time than that of the PLA/CNTs membrane, due to better capacitance performance. Heat treatment at the Tg of PLA for 2 hours contributed to the maximum specific capacitance of 510 Fg^{-1}, as shown in Figure **33** [70].

5. CONCLUSIONS AND PERSPECTIVE

This snapshot review summarized the r ecent progress of the PLA composites modified with CNT in emerging field. Especially, various preparation methods including melt blending, solution blending, in-situ polymerization, mechanochemical method, 3D printing and physical foaming were used to prepare various PLA composite materials with versatile micro- structures and excellent properties. Also, emerging application scenarios of the CNT/PLA composites have been summarized.

In future, more and more facile preparation methods and eco-friendly manufacture processes will be developed to prepare diverse functional CNT/PLA composite materials, which will give a green light to extend the use of this sustainable composite materials.

ACKNOWLEDGMENTS

The authors thank the financial support from the Education Department of the Shaanxi Provincial Government (No.: 22JC038).

CONFLICTS OF INTEREST

The authors have no conflicts of interest to declare.

REFERENCES

[1] R. Geyer, J.R. Jambeck, K.L. Law, Production, use, and fate of all plastics ever made, Sci Adv 3(7) (2017). https://doi.org/10.1126/sciadv.1700782

[2] F. Qian, R. Jia, M. Cheng, A. Chaudhary, S. Melhi, S.D. Mekkey, N. Zhu, C. Wang, F. Razak, X. Xu, C. Yan, X. Bao, Q. Jiang, J. Wang, M. Hu, An overview of polylactic acid (PLA) nanocomposites for sensors, Adv Compos Hybrid Mater 7(3) (2024) 75. https://doi.org/10.1007/s42114-024-00887-6

[3] N. Shekhar, A. Mondal, Synthesis, properties, environmental degradation, processing, and applications of polylactic acid

(PLA): An overview, Polym Bull (2024). https://doi.org/10.1007/s00289-024-05252-7

[4] T. Qiang, Y. Chou, H. Gao, Environmental impacts of styrene-butadiene-styrene toughened wood fiber/polylactide composites: A cradle-to-gate life cycle assessment, Int J Env Res Pub Health 16(18) (2019). https://doi.org/10.3390/ijerph16183402

[5] T. Qiang, J. Wang, M.P. Wolcott, Facile preparation of cellulose/polylactide composite materials with tunable mechanical properties, Polym-Plast Technol 57(13) (2018) 1288-1295. https://doi.org/10.1080/03602559.2017.1381243

[6] T. Qiang, J. Wang, P.M. Wolcott, Facile fabrication of 100% bio-based and degradable ternary cellulose/PHBV/PLA composites, Materials 11(2) (2018). https://doi.org/10.3390/ma11020330

[7] H. Gao, T. Qiang, Fracture surface morphology and impact strength of cellulose/PLA composites, Materials 10(6) (2017). https://doi.org/10.3390/ma10060624

[8] V.O. Bulatovi, V. Mandi, D.K. Grgi, A. Ivani, Biodegradable polymer blends based on thermoplastic starch, J Polym Environ 29(2) (2021). https://doi.org/10.1007/s10924-020-01874-w

[9] L. Bouapao, H. Tsuji, K. Tashiro, J. Zhang, M. Hanesaka, Crystallization, spherulite growth, and structure of blends of crystalline and amorphous poly(lactide)s, Polymer 50(16) (2009) 4007-4017. https://doi.org/10.1016/j.polymer.2009.06.040

[10] M.F.L. De Volder, S.H. Tawfick, R.H. Baughman, A.J. Hart, Carbon nanotubes: Present and future commercial applications, Science 339(6119) (2013) 535-539. https://doi.org/10.1126/science.1222453

[11] Z. Spitalsky, D. Tasis, K. Papagelis, C. Galiotis, Carbon nanotube-polymer composites: Chemistry, processing, mechanical and electrical properties, Prog Polym Sci 35(3) (2010) 357-401. https://doi.org/10.1016/j.progpolymsci.2009.09.003

[12] Z. Han, A. Fina, Thermal conductivity of carbon nanotubes and their polymer nanocomposites: A review, Prog Polym Sci 36(7) (2011) 914-944. https://doi.org/10.1016/j.progpolymsci.2010.11.004

[13] S. Barrau, C. Vanmansart, M. Moreau, A. Addad, G. Stoclet, J.M. Lefebvre, R. Seguela, Crystallization behavior of carbon nanotube-polylactide nanocomposites, Macromolecules 44(16) (2011) 6496-6502. https://doi.org/10.1021/ma200842n

[14] X. Zhao, J. Yu, X. Wang, Z. Huang, W. Zhou, S. Peng, Strong synergistic toughening and compatibilization enhancement of carbon nanotubes and multi-functional epoxy compatibilizer in high toughened polylactic acid (PLA)/poly (butylene adipate-co-terephthalate) (PBAT) blends, Int J Biol Macromol 250 (2023) 126204. https://doi.org/10.1016/j.ijbiomac.2023.126204

[15] H. Barangizi, J. Krajenta, A. Pawlak, The influence of entanglements of macromolecules on the mechanical and thermal properties of polylactide composites with carbon nanotubes, Express Polym Lett 17(7) (2023) 738-758. https://doi.org/10.3144/expresspolymlett.2023.55

[16] L. Pan, Q. Lv, N. Xu, Properties and mechanism of antistatic biodegradable polylactic acid/multi-walled carbon nanotube composites, J Eng Fiber Fabr 15 (2020). https://doi.org/10.1177/1558925020968813

[17] Y. Zhou, L. Lei, B. Yang, J. Li, J. Ren, Preparation and characterization of polylactic acid (PLA) carbon nanotube nanocomposites, Polym Test 68 (2018) 34-38. https://doi.org/10.1016/j.polymertesting.2018.03.044

[18] T. Qiang, X. Qi, H. Gao, H. Qiang, S. Wang, L. Hu, N. Hu, UV-shielding, flexible and enhanced thermal- conductive polylactide composites modified with single-layered, large-sized MXene nano-sheets, Polym Bull (2024). https://doi.org/10.1007/s00289-024-05303-z

[19] K.D.M. Nayara, F.M. Eduardo, L.M.S.O. Rodrigo, A.W.D.B. Idália, P.B.M. João, E. Elisa, S.A. Suelen, M.R.D.V. Luana, R.P. Fabio, D.S.T. Eliandra, Synergistic effect of adding bioglass and carbon nanotubes on poly (lactic acid) porous membranes for guided bone regeneration, Mater Sci Eng C 117 (2020). https://doi.org/10.1016/j.msec.2020.111327

[20] S. Yang, J. Xu, Y. Li, J. Lei, G. Zhong, R. Wang, Z. Li, Effects of solvents on stereocomplex crystallization of high-molecular-weight polylactic acid racemic blends in the presence of carbon nanotubes, Macromol Chem Phys 218(21) (2017). https://doi.org/10.1002/macp.201700292

[21] R. Cui, K. Jiang, M. Yuan, J. Cao, L. Lin, Z. Tang, Y. Qin, Antimicrobial film based on polylactic acid and carbon nanotube for controlled cinnamaldehyde release, J Mater Res Technol 9(5) (2020) 10130-10138. https://doi.org/10.1016/j.jmrt.2020.07.016

[22] B. Yu, Z. Zhao, S. Fu, L. Meng, Y. Liu, F. Chen, K. Wang, Q. Fu, Fabrication of PLA/CNC/CNT conductive composites for high electromagnetic interference shielding based on Pickering emulsions method, Compos Part A 125 (2019) 105558. https://doi.org/10.1016/j.compositesa.2019.105558

[23] Q. Li, Q. Zhou, D. Deng, Q. Yu, L. Gu, K. Gong, K. Xu, Enhanced thermal and electrical properties of poly(D,L-lactide)/multi-walled carbon nanotubes composites by in-situ polymerization, T Nonferr Metal Soc 23(5) (2013) 1421-1427. https://doi.org/10.1016/S1003-6326(13)62612-6

[24] Q. Wang, H. Wang, P. Du, J. Liu, D. Liu, P. Liu, Porous polylactic acid/carbon nanotubes/polyaniline composite film as flexible free-standing electrode for supercapacitors, Electrochim ACTA 294 (2019) 312-324. https://doi.org/10.1016/j.electacta.2018.10.108

[25] K.J. Ardila-Fierro, J.G. Hernandez, Sustainability assessment of mechanochemistry by using the twelve principles of green chemistry, ChemSusChem 14(10) (2021) 2145-2162. https://doi.org/10.1002/cssc.202100478

[26] E.M. Lloyd, J.R. Vakil, Y. Yao, N.R. Sottos, S.L. Craig, Covalent mechanochemistry and contemporary polymer network chemistry: A marriage in the making, J Am Chem Soc 145(2) (2023) 751-768. https://doi.org/10.1021/jacs.2c09623

[27] J. Li, C. Nagamani, J.S. Moore, Polymer mechanochemistry: From destructive to productive, Accounts Chem Res 48(8) (2015) 2181-2190. https://doi.org/10.1021/acs.accounts.5b00184

[28] □淳, 付豪, □昌□, □敏, 李怡俊, 固相力化学反□器制□聚乳酸/碳□米管□米复合材料及性能研究, 化工新型材料 49(12) (2021) 89-92. https://doi.org/10.12677/MS.2022.124040

[29] T.M. Joseph, A. Kallingal, A.M. Suresh, D.K. Mahapatra, M.S. Hasanin, J. Haponiuk, S. Thomas, 3D printing of polylactic acid: recent advances and opportunities, Int J Adv Manuf Tech 125(3-4) (2023) 1015-1035. https://doi.org/10.1007/s00170-022-10795-y

[30] Z. Liu, Y. Wang, B. Wu, C. Cui, Y. Guo, C. Yan, A critical review of fused deposition modeling 3D printing technology in manufacturing polylactic acid parts, Int J Adv Manuf Tech 102(9-12) (2019) 2877-2889. https://doi.org/10.1007/s00170-019-03332-x

[31] J. Liu, L. Sun, W. Xu, Q. Wang, S. Yu, J. Sun, Current advances and future perspectives of 3D printing natural-derived biopolymers, Carbohyd Polym 207 (2019) 297-316. https://doi.org/10.1016/j.carbpol.2018.11.077

[32] X. Li, G. Zhang, W. Li, Z. Yu, K. Yang, H. Lan, The electric-field-driven fusion jetting 3D printing for fabricating high resolution polylactic acid/multi-walled carbon nanotube composite micro-scale structures, Micromachines 11(12) (2020). https://doi.org/10.3390/mi11121132

[33] S. Shi, Z. Peng, J. Jing, L. Yang, Y. Chen, 3D printing of delicately controllable cellular nanocomposites based on polylactic acid incorporating graphene/carbon nanotube hybrids for efficient electromagnetic interference shielding, ACS Sustain Chem Eng 8(21) (2020) 7962-7972. https://doi.org/10.1021/acssuschemeng.0c01877

[34] W. Liu, X. Zhu, H. Gao, X. Su, X. Wu, Preparation and characterization of PLA foam chain extended through grafting octa(epoxycyclohexyl) POSS onto carbon nanotubes, Cell Polym 39(3) (2020) 117-137. https://doi.org/10.1177/0262489320912521

[35] L. Yang, Y. Dexian, L. Wei, Z. Hongfu, Z. Yuxia, W. Xiangdong, Fabrication of biodegradable poly (lactic acid)/carbon nanotube nanocomposite foams: Significant improvement on rheological property and foamability, Int J Biol Macromol 163 (2020). https://doi.org/10.1016/j.ijbiomac.2020.07.094

[36] I. Montes-Zavala, E.O. Castrejon-Gonzalez, G. Sanchez-Balderas, E. Perez, J.A. Gonzalez-Calderon, Effect of H bonds on thermal behavior and cohesion in polylactic acid nanocomposites and nitrogen- doped carbon nanotubes, J MATER SCI 55(8) (2020) 3354-3368. https://doi.org/10.1007/s10853-019-04245-6

[37] C. Hu, Z. Li, Y. Wang, J. Gao, K. Dai, G. Zheng, C. Liu, C. Shen, H. Song, Z. Guo, Comparative assessment of the strain-sensing behaviors of polylactic acid nanocomposites: reduced graphene oxide or carbon nanotubes, J Mater Chem C 5(9) (2017) 2318-2328. https://doi.org/10.1039/C6TC05261D

[38] □琦, 权慧, 刘建叶, 高达利, □□□, 改性碳□米管增强聚乳酸复合材料的制□及其性能, 合成□脂及塑料 39(2) (2022) 5-10+24.

[39] R. Kotsilkova, S. Tabakova, R. Ivanova, Effect of graphene nanoplatelets and multiwalled carbon nanotubes on the viscous and viscoelastic properties and printability of polylactide nanocomposites, Mech Time-Depend Mat (2021). https://doi.org/10.1007/s11043-021-09503-2

[40] G.M. Neelgund, A. Oki, Contribution of polylactic acid and Pd nanoparticles in the enhanced photothermal effect of carbon nanotubes, ChemistrySelect 5(35) (2020) 11020-11028. https://doi.org/10.1002/slct.202003191

[41] W. Liu, X. Wu, S. Liu, X. Cheng, C. Zhang, CNT@LDH functionalized poly(lactic acid) membranes with super oil-water separation and real-time press sensing properties, Polym Compos 43(9) (2022) 6548-6559. https://doi.org/10.1002/pc.26968

[42] C. Kuan, C. Chen, H. Kuan, K. Lin, Multi-walled carbon nanotube reinforced poly (L-lactic acid), J Phys Chem Solids 69 (2008) 1399-1402. https://doi.org/10.1016/j.jpcs.2007.10.061

[43] C. Teng, C.M. Ma, B. Cheng, Y. Shih, J. Chen, Y. Hsiao, Mechanical and thermal properties of polylactide-grafted vapor-grown carbon nanofiber/polylactide nanocomposites, Compos Part A 42(8) (2011) 928-934. https://doi.org/10.1016/j.compositesa.2011.03.021

[44] S. Wang, Y. Wu, Y. Cheng, W. Hu, The development of polylactic acid/multi-wall carbon nanotubes/polyethylene glycol scaffolds for bone tissue regeneration application, Polymers 13(11) (2021). https://doi.org/10.3390/polym13111740

[45] T. Vu, P. Nikaeen, M. Akobi, D. Depan, W. Chirdon, Enhanced nucleation and crystallization in PLA/CNT composites via disperse orange 3 with corresponding improvement in nanomechanical properties, Polym Advan Technol 31(3) (2020) 415-424. https://doi.org/10.1002/pat.4777

[46] T. Makowski, M. Svyntkivska, E. Piorkowska, D. Kregiel, Multifunctional polylactide nonwovens with 3D network of multiwall carbon nanotubes, Appl Surf Sci 527 (2020). https://doi.org/10.1016/j.apsusc.2020.146898

[47] L. Wang, J. Qiu, E. Sakai, Mechanical and electrical properties of polylactic acid/carbon nanotube composites by rolling process, Sci Eng Compos Mater 25(5) (2018) 891-901. https://doi.org/10.1515/secm-2017-0113

[48] F. Zhang, W. Jiang, X. Song, J. Kang, Y. Cao, M. Xiang, Effects of hyperbranched polyester-modified carbon nanotubes on the crystallization kinetics of polylactic acid, ACS Omega 6(15) (2021) 10362-10370. https://doi.org/10.1021/acsomega.1c00738

[49] B. Tiantian, Z. Bo, L. Hu, W. Yaming, S. Gang, L. Chuntai, S. Changyu, Biodegradable poly(lactic acid) nanocomposites reinforced and toughened by carbon nanotubes/clay hybrids, Int J Biol Macromol 151 (2020) 628-634. https://doi.org/10.1016/j.ijbiomac.2020.02.209

[50] Y. Zare, K.Y. Rhee, Following the morphological and thermal properties of PLA/PEO blends containing carbon nanotubes (CNTs) during hydrolytic degradation, Compos Part B 175 (2019) 107132. https://doi.org/10.1016/j.compositesb.2019.107132

[51] M. Svyntkivska, T. Makowski, E. Piorkowska, M. Brzezinski, A. Herc, A. Kowalewska, Modification of polylactide nonwovens with carbon nanotubes and ladder poly(silsesquioxane), Molecules 26(5) (2021). https://doi.org/10.3390/molecules26051353

[52] R. Scaffaro, A. Maio, Integrated ternary bionanocomposites with superior mechanical performance via the synergistic role of graphene and plasma treated carbon nanotubes, Compos Part B 168 (2019) 550- 559. https://doi.org/10.1016/j.compositesb.2019.03.076

[53] O.M. Sanusi, A. Benelfellah, L. Papadopoulos, Z. Terzopoulou, L. Malletzidou, I.G. Vasileiadis, K. Chrissafis, D.N. Bikiaris, H.N. Aït, Influence of montmorillonite/carbon nanotube hybrid nanofillers on the properties of poly(lactic acid), Appl Clay Sci 201 (2020) 105925. https://doi.org/10.1016/j.clay.2020.105925

[54] P. Szatkowski, L. Czechowski, J. Gralewski, M. Szatkowska, Mechanical properties of polylactide admixed with carbon nanotubes or graphene nanopowder, Materials 14(20) (2021). https://doi.org/10.3390/ma14205955

[55] J. Urquijo, N. Aranburu, S. Dagréou, G. Guerrica-Echevarría, J.I. Eguiazábal, CNT-induced morphology and its effect on properties in PLA/PBAT-based nanocomposites, Eur Polym J 93 (2017) 545-555. https://doi.org/10.1016/j.eurpolymj.2017.06.035

[56] Z. Bo, B. Tiantian, W. Pan, W. Yaming, L. Chuntai, S. Changyu, Selective dispersion of carbon nanotubes and nanoclay in biodegradable poly(ε-caprolactone)/poly(lactic acid) blends with improved toughness, strength and thermal stability, Int J Biol Macromol 153 (2020) 1272-1280. https://doi.org/10.1016/j.ijbiomac.2019.10.262

[57] Y. Wang, Y. Mei, Q. Wang, W. Wei, F. Huang, Y. Li, J. Li, Z. Zhou, Improved fracture toughness and ductility of PLA composites by incorporating a small amount of surface-modified helical carbon nanotubes, Compos Part B 162 (2019) 54-61. https://doi.org/10.1016/j.compositesb.2018.10.060

[58] C. Yang, T. Huang, J. Yang, N. Zhang, Y. Wang, Z. Zhou, Carbon nanotubes induced brittle-ductile transition behavior of the polypropylene/ethylene-propylene-diene terpolymer blends, Compos Sci Technol 139 (2017) 109-116. https://doi.org/10.1016/j.compscitech.2016.12.016

[59] Y.Y. Shi, W.B. Zhang, J.H. Yang, T. Huang, N. Zhang, Y. Wang, G.P. Yuan, C.L. Zhang, Super toughening of the poly(L-lactide)/thermoplastic polyurethane blends by carbon nanotubes, RSC Adv 3 (2013) 26271. https://doi.org/10.1039/c3ra43253j

[60] A.P.B. Silva, L.S. Montagna, F.R. Passador, M.C. Rezende, A.P. Lemes, Biodegradable nanocomposites based on PLA/PHBV blend reinforced with carbon nanotubes with potential for electrical and electromagnetic applications, Express Polym Lett 15(10) (2021) 987-1003. https://doi.org/10.3144/expresspolymlett.2021.79

[61] E.J. Dil, M. Arjmand, I.O. Navas, U. Sundararaj, B.D. Favis, Interface bridging of multiwalled carbon nanotubes in polylactic acid/poly(butylene adipate-co-terephthalate): Morphology, rheology, and electrical conductivity, Macromolecules 53(22) (2020) 10267-10277. https://doi.org/10.1021/acs.macromol.0c01525

[62] E.C. Lopes Pereira, M.E.C. Fernandes Da Silva, K. Pontes, B.G. Soares, Influence of protonic ionic liquid on the dispersion of carbon nanotube in PLA/EVA blends and blend compatibilization, Front Mater 6 (2019) 234. https://doi.org/10.3389/fmats.2019.00234

[63] Y. Wang, Z. Fan, H. Zhang, J. Guo, D. Yan, S. Wang, K. Dai, Z. Li, 3D-printing of segregated carbon nanotube/polylactic acid composite with enhanced electromagnetic interference shielding and mechanical performance, Mater Design 197 (2021). https://doi.org/10.1016/j.matdes.2020.109222

[64] N. H., K. Y., Elucidating the plasticizing effect on mechanical and thermal properties of poly(lactic acid)/carbon nanotubes nanocomposites, Polym Bull 78(12) (2020). https://doi.org/10.1007/s00289-020-03471-2

[65] X.H. Gao, D. Xie, C. Yang, Effects of a PLA/PBAT biodegradable film mulch as a replacement of polyethylene film and their residues on crop and soil environment, Agric Water Manage 255 (2021) 107053. https://doi.org/10.1016/j.agwat.2021.107053

[66] T. Vu, P. Nikaeen, W. Chirdon, A. Khattab, D. Depan, Improved weathering performance of poly(lactic acid) through carbon nanotubes addition: Thermal, microstructural, and nanomechanical analyses, Biomimetics 5(4) (2020). https://doi.org/10.3390/biomimetics5040061

[67] □□, □□□, 高国金, 明津法, 黄□□, 王雪芳, 王娜, 宁新, 碳□米管含量□聚乳酸/碳□米管□□ □□膜性能的影响, 毛□科技 50(8) (2022) 98-103. https://doi.org/10.3788/CJL202249.0202301

[68] S. Liu, G. Wu, X. Chen, X. Zhang, J. Yu, M. Liu, Y. Zhang, P. Wang, Degradation behavior in vitro of carbon nanotubes (CNTs)/poly(lactic acid) (PLA) composite suture, Polymers 11(6) (2019). https://doi.org/10.3390/polym11061015

[69] L. Gan, A. Geng, L. Jin, Q. Zhong, L. Wang, L. Xu, C. Mei, Antibacterial nanocomposite based on carbon nanotubes-silver nanoparticles-co-doped polylactic acid, Polym Bull 77(2) (2020) 793-804. https://doi.org/10.1007/s00289-019-02776-1

[70] V. Gupta, F. Alam, P. Verma, A.M. Kannan, S. Kumar, Additive manufacturing enabled, microarchitected, hierarchically porous polylactic-acid/lithium iron phosphate/carbon nanotube nanocomposite electrodes for high performance Li-Ion batteries, J Power Sources 494 (2021). https://doi.org/10.1016/j.jpowsour.2021.229625

Received on 30-05-2024 Accepted on 29-07-2024 Published on 12-08-2024

DOI: https://doi.org/10.12974/2311-8717.2024.12.03